Cooperative Vehicular Ad-hoc Transmission for LTE-A MIMO-Downlink Using Amplify-and-Forward Relaying

Mohamed F. Feteiha and Hossam S. Hassanein
Telecommunications Research Lab (TRL)
School of Computing
Queen's University
Kingston, Ontario, Canada, K7L 3N6
Email:{feteiha, hossam}@cs.queensu.ca

***Abstract*—Cooperative communication has been recently applied to vehicular networks to enable coverage extension and enhance link reliability through distributed spatial diversity. In this paper, we investigate the performance of cooperative vehicular relaying over a *doubly-selective* (i.e., *frequency-selective* and *time-selective*) fading channel for an LTE-Advanced downlink session. Using Amplify-and-Forward (AF) relaying with orthogonal cooperation protocol and Multiple-Input Multiple-Output (MIMO) deployment at the source and destination, we derive a pairwise error probability (PEP) expression and demonstrate the achievable diversity gains. Space-Time Block Coding (STBC) is used to ensure the orthogonality of the transmitted-received signals. Our results demonstrate that, via proper linear precoding constellation, the proposed cooperative-MIMO vehicular relaying is capable of extracting the maximum available diversity in frequency (through multipath diversity), time (through Doppler diversity) and space (through cooperative diversity as well as the MIMO deployment) dimensions. We further conduct numerical simulations to confirm the analytical derivations and present the error rate performance of the cooperative relaying vehicular scheme under consideration.**

I. Introduction

Vehicular ad hoc networks supporting both Vehicle-to-Vehicle (V2V) and Vehicle-to-Infrastructure (V2I) communication have been extensively investigated for diverse applications. Although vehicular applications are of special interest, achieving the required high reliability propagation environments necessitates further improvements of the physical layer aspects due to the rapid topology changes. Indeed, dynamic road conditions and vehicular characteristics affect connectivity in vehicular networks. Recently there has been increased interest in using vehicles as relaying terminals to extend the transmission range using a simple and energy efficient technique, by enabling its ad-hoc connectivity, and by taking advantage of the dense availability to enhance link reliability through distributed spatial diversity [1]. Most of the previous studies have addressed the design of upper layer protocols and related challenges in vehicular networks. For example, in [2], a link scheduling scheme has been investigated to maximize the throughput for a cooperative vehicular network with Amplify-and-Forward (AF) relaying. In [3], a cross layer routing approach has been studied to overcome the challenge of frequent path disruptions caused by high speed mobility of vehicles. In [4], a delay-tolerant routing method has been proposed to enhance the robustness of routing in a cooperative vehicular network with decode-and-forward (DF) relaying. In [5], so-called Cookie-Cooperative Automatic Repeat reQuest (CCARQ) mechanism has been proposed to improve network performance by repairing intermittent broken connections in an AF-based cooperative vehicular network. A relatively small number of current works, i.e. [6], have focused on the physical layer issues of cooperative vehicular networks and these existing works mainly build upon the rather simplifying assumption of frequency-flat and quasi-static fading channels.

In an earlier work [7], we investigated the performance gains of a transmission scheme in Long Term Evaluation -Advanced (LTE-A) networks located in an urban area where vehicles act as selected best-relaying cooperating terminals between a highly elevated BS and a stationary end-user. DF relaying with a single antenna deployment at the communicating nodes is assumed. Analytical and simulation results demonstrated significant performance gains. In [8], we extended vehicular cooperation into downlink LTE-A networks, where vehicles act as relaying terminals between eNodeB/BS and receiver equipment mounted on another traveling vehicle. PEP were derived, and performance results show that, through proper precoding, the proposed system is able to extract maximum diversity in time, frequency and space.

Due to the envisaged high mobility defined in LTE-A systems and changing road conditions, a technology which supports scattering and diversity to improve network performance is needed. Hence, we propose using the MIMO wireless communication technology at sender and receiver. MIMO has the potential to improve the cooperative network accessibility by providing significant diversity gains with the use of a modified STBC. As a result of intensive studies of MIMO techniques over the last decade, the family of STBC provides substantial diversity gains without any bandwidth extension. In our proposed cooperative-MIMO deployment, a transmission scheme in LTE-A networks where vehicles act as relaying cooperating terminals for eNodeB-to-Vehicle downlink is assumed. To overcome the performance degradation resulting from the associated wireless links that are characterized by a doubly-selective fading channel, we deploy a precoded cooperative transmission technique to extract the underlying rich multipath-Doppler diversity. Further, for extra spatial diversity we consider that the source and destination nodes are equipped with two antennas while the relay node has

978-1-4799-1353-4/13/$31.00 ©2013 IEEE

a single transmit/receive antenna. We modify the Alamouti-type STBC [9] to be used across the two transmit antennas of the source node. Digital phase sweeping (DPS) is deployed to mitigate the distortion of the STBC orthogonality resulting from the time-selectivity effects of the associated channel [10].

We propose an effective coding transmission scheme, derive PEP expressions to assess our analysis and future research studies of such an approach and demonstrate the achievable diversity gains. Our analytical and simulation results show that significant diversity gains through the precoding transmission and MIMO deployment are achievable. Results also show great reduction in error rates, and required transmitting power compared to traditional transmission schemes.

The paper is organized as follows. In Section II, we present the precoded cooperative system model along with the vehicular fading channel. In Section III, we provide diversity gain analysis through PEP derivation. In Section IV, we present the numerical simulation results for the error rate performance. We conclude our findings in Section V.

Notations: $(.)^{\mathrm{T}}$, $(.)^{*}$ and $(.)^{\mathrm{H}}$ denotes transpose, conjugate and Hermitian operations, respectively. $\mathbb{E}[.]$, $|.|$ and $\otimes$ denotes expectation, absolute value and Kronecker product, respectively. $[\mathbf{H}]_{k,m}$ represents the (k,m)-th entry of $\mathbf{H}$. $\mathbf{I}_N$ indicates an $N \times N$-size identity matrix. $\mathbf{0}$ represents all-zeros matrix with proper dimensions. $\lceil . \rceil$ and $\lfloor . \rfloor$ denotes integer ceil and integer floor operations, respectively. $*$ is the convolution operator. **Bold** letters/symbols denote the matrices and vectors.

II. System Model

We consider an LTE-A downlink session in a highway where the destination and a relaying vehicles are travelling in the same direction with similar speeds and surrounded by scatterers. First we describe the channel model and then present the cooperative MIMO scheme under consideration.

A. Channel Model

To reflect the relay geometry, we consider an aggregate channel model which takes into account both path-loss and small-scale fading. The path loss is proportional to d^{α} where d is the propagation distance and α is the path loss coefficient. Let d_{sd}, d_{sr} and d_{rd} denote the distances of source-to-destination (S→D), source-to-relay (S→R), and relay-to-destination (R→D) links, respectively, and θ is the angle between lines S→R and R→D. Normalizing the path loss in S→D to be unity, the relative geometrical gains are defined respectively as $G_{sr} = (d_{sd}/d_{sr})^{\alpha}$ and $G_{rd} = (d_{sd}/d_{rd})^{\alpha}$. The ratio G_{sr}/G_{rd} reflects the effect of relay location. More negative this ratio is, more closely the relay is placed to destination terminal. For the short-term fading model, we adopt the double-ring channel model of which assumes that scatterers lay uniformly over two rings around the two vehicles. The envelope of this channel follows a Rayleigh distribution with an autocorrelation function represented by the double-ring channel model [11]

$$C(\tau) = \sigma^2 J_0\left((2\pi/\lambda)\, v_1 \tau\right) J_0\left((2\pi/\lambda)\, v_2 \tau\right) \qquad (1)$$

where $J_0(.)$ is the zero order Bessel function, σ^2 is the channel variance, while v_1 and v_2 are the two maximum speeds for the two communicating terminals. The maximum Doppler shift due to the relative motion of the two vehicles $f_{D_m} = [v_1 \cos(\vartheta_1) + v_2 \cos(\vartheta_2)]/\lambda$, where λ is the wavelength of the carrier frequency with ϑ_1 and ϑ_2 representing the angle of incidence of the signal on the first and second vehicles, respectively. Maximum Doppler shift f_{D_m} is calculated based on the maximum velocities experienced. We can further define the Doppler spread given by $f_d = 1/T_d$, where T_d is the coherence time of the channel. Besides time-selectivity, the channel is subject to frequency-selectivity quantified through delay spread τ_d.

We consider a highway traffic scenario, where the relay and destination vehicles are assumed to be traveling in the same direction with similar speeds and communicating with a fixed BS through LTE-A downlink session. This results in a relative velocity nearly equal to zero and leads to time-flat and frequency-flat fading in the R→D link, and doubly-selective fading channel in the S→R link. We adopt the orthogonal cooperation protocol in [12] and Amplify-and-Forward (AF) relaying. In the broadcasting phase, the BS sends its signal to the relay and the destination vehicles. In the relaying phase, the relay vehicle properly amplify its received signal and forward it to the designated vehicle. The destination makes its decision based on the maximum likelihood (ML) detection of the two received signals. Fig-1 shows the block diagram for the source and the destination with $\mathcal{M}_2$ denoting the STBC matrix. As summarized in Table-1, we use four transmission phases. For ease of presentation, first we provide the received signals for the single antenna-to-antenna links. We consider a precoded cooperative scheme, the input data blocks (generated from an M-QAM constellation) of length N_t are divided into shorter sub-blocks of length N_s ($N_s \leq N_t$). Let each of these sub-blocks be denoted by $\mathbf{s}(n)$ which will be the input to the linear precoder $\mathbf{\Theta}$ of size $N_s \times N_t$. We use the precoder proposed

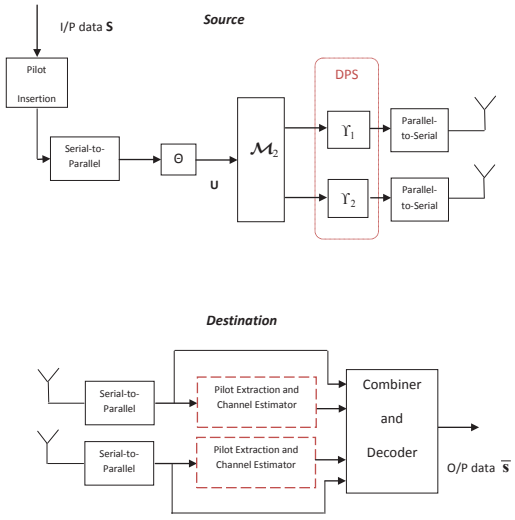

Fig. 1: Alamouti-code based MIMO cooperative transmission.

TABLE I: Encoding for STBC cooperative transmission.

	(Phase 1) broadcast-1	(Phase 2) broadcast-2	(Phase 3) relaying-1	(Phase 4) relaying-2
Tx antenna-1	transmit $\mathbf{s}(n-1)$	transmit $-\mathbf{s}^*(n)$	*idle*	*idle*
Tx antenna-2	transmit $\mathbf{s}(n)$	transmit $\mathbf{s}^*(n-1)$	*idle*	*idle*
Relay antenna	receive $\mathbf{y}_{sr}(n-1)$	receive $\mathbf{y}_{sr}(n)$	transmit $\bar{\mathbf{y}}_{sr}(n-1)$	transmit $\bar{\mathbf{y}}_{sr}(n)$
Rx antenna-1	receive $\mathbf{y}_{sd,1}(n-1)$	receive $\mathbf{y}_{sd,1}(n)$	receive $\mathbf{y}_{rd,1}(n-1)$	receive $\mathbf{y}_{rd,1}(n)$
Rx antenna-2	receive $\mathbf{y}_{sd,2}(n-1)$	receive $\mathbf{y}_{sd,2}(n)$	receive $\mathbf{y}_{rd,2}(n-1)$	receive $\mathbf{y}_{rd,2}(n)$

in [13] which ensures the maximum diversity over doubly-selective channels and eliminates the inter-block interference (IBI) term. It is given by $\mathbf{\Theta} = \mathbf{F}_{P+Q}^{\mathrm{H}} \mathbf{T_1} \otimes \mathbf{T_2}$ where $\mathbf{F}_{P+Q}^{\mathrm{H}}$ is a $(P+Q)$-point IFFT matrix, $\mathbf{T}_1 := [\mathbf{I}_P,\ \mathbf{0}_{P\times Q}]^{\mathrm{T}}$ and $\mathbf{T}_2 := [\mathbf{I}_Z,\ \mathbf{0}_{Z\times L}]^{\mathrm{T}}$. Here, $P \geq 1$ and $Z \geq 1$ are the precoder design parameters such that $N_s = PZ$, $N_t = (P+Q)(Z+L)$. We have $L = \lceil \tau_d / T_s \rceil$ as the number of the resolvable multipath components and the number of Doppler shifts experienced over the data block is given by $Q = \lceil N_t T_s f_{D_m} \rceil$.

The OFDM signals converted to frequency domain by implementing discrete Fourier transform (DFT) are given by

$$s(\ell) = \left(1/\sqrt{N}\right) \sum_{k=0}^{N-1} x(k)\, e^{-jw_k} \tag{2}$$

where $w_k = 2\pi\ell k/N$, while $x(k)$ is the modulated symbol, and $n = 0, \ldots, N-1$. The Basis Expansion Model (BEM) is used to model the associated doubly-selective channel, and is given by

$$h_B(\ell; l) = \sum_{q=0}^{Q} h_q(n; l)\, e^{jw_q}, l \in [0, L] \tag{3}$$

where $w_q = 2\pi\ell(q - Q/2)/N_s$ is the finite Fourier bases that capture the time variation, $h_q(n; l)$ is zero-mean complex Gaussian. Here, ℓ denotes the serial index for the input data symbols. The block index is given by $n = \lfloor \ell / N_t \rfloor$. Define $\mathbf{H}_{sd,q}^{(0)}$, $\mathbf{H}_{sr,q}^{(0)}$ and $\mathbf{H}_{rd,q}^{(0)}$ as the lower triangular Toeplitz channel matrices with entries given by (3). Let L_{sd}, L_{sr}, and L_{rd} denote the channel multipath orders for the S→D, S→R, and R→D links, respectively. Further, let Q_{sd}, Q_{sr}, and Q_{rd} denote the number of resolvable Doppler components and define $\mathrm{Q} = \max(Q_{sd}, Q_{sr}, Q_{rd})$.

In the broadcasting phase, the received signals at the relay can be expressed in a matrix form as

$$\begin{aligned} \mathbf{y}_{sr}(n) &= \sqrt{G_{sr}E_s} \sum_{q=0}^{\mathrm{Q}} \mathbf{D}(w_q) \mathbf{H}_{sr,q}^{(0)}(n)\, \mathbf{u}(n) + \mathbf{n}_{sr}(n) \\ &= \sqrt{G_{sr}E_s} \mathbf{\Phi}(n)\, \mathbf{h}_{sr}(n) + \mathbf{n}_{sr}(n) \end{aligned} \tag{4}$$

where $\mathbf{u}(n) = \mathbf{\Theta}\mathbf{s}(n)$ is the transmitted data block, E_s is the modulation symbol energy, $\mathbf{D}(w_q) := \mathrm{diag}\left[\ 1,\ \ldots\ \exp(jw_q(N_t-1))\ \right]$ and $\mathbf{n}_{sr}(n)$ is the additive white Gaussian noise (AWGN) vector with entries of zero mean and $N_0/2$ variance. The second equality follows from the commutativity of products of Toeplitz matrices with vectors where we have further defined the augmented matrices $\mathbf{h}_{sr}(n) = \left[\ \mathbf{h}_{sr,0}^{\mathrm{T}}(n),\ \ldots\ , \mathbf{h}_{sr,\mathrm{Q}}^{\mathrm{T}}(n)\ \right]^{\mathrm{T}}$ and $\mathbf{\Phi}(n) = \left[\ \mathbf{D}(w_0)\mathbf{U}(n),\ \ldots\ , \mathbf{D}(w_{\mathrm{Q}})\mathbf{U}(n)\ \right]$, with $\mathbf{U}$ denoting the lower triangular Toeplitz matrix. Similarly, the received signal at the destination can be written as

$$\mathbf{y}_{sd}(n) = \sqrt{E_s} \mathbf{\Phi}(n)\, \mathbf{h}_{sd}(n) + \mathbf{n}_{sd}(n) \tag{5}$$

where $\mathbf{h}_{sd}(n) = \left[\ \mathbf{h}_{sd,0}^{\mathrm{T}}(n),\ \ldots\ , \mathbf{h}_{sd,\mathrm{Q}}^{\mathrm{T}}(n)\ \right]^{\mathrm{T}}$ and $\mathbf{n}_{sd}(n)$ is the AWGN vector with entries of zero mean and $N_0/2$ variance.

The relay scales the received signal $\mathbf{y}_{sr}(n)$ (to ensure that an average output power is maintained) by a factor of $\sqrt{\mathbb{E}_{\mathbf{n}_{sr},\mathbf{\Phi}}[|\mathbf{y}_{sr}(n)|^2]} = \left(G_{sr}E_s^2\right) \mathrm{tr}\left(\mathbb{E}[\mathbf{\Phi}^{\mathrm{H}}(n)\mathbf{\Phi}(n)]\right) + N_t(N_0/2)$, then forwards the resulting signal to the destination. At the destination, after a proper normalization [14], we have the resulting signal as

$$\mathbf{y}_{rd}(n) = K(n) \sqrt{E_s} \mathbf{\Phi}_{srd}(n)\, \mathbf{h}_{srd}(n) + \mathbf{n}_{srd}(n) \tag{6}$$

where

$$K(n) = \sqrt{G_{sr}G_{rd}E_s} \Big/ \left(\mathbf{\Omega}(n)\, \mathbb{E}_{\mathbf{n}_{sr},\mathbf{\Phi}}\left[|\mathbf{y}_{sr}(n)|^2\right]\right),$$

$$\mathbf{\Phi}_{srd}(n) = \sum\nolimits_{q_2=0}^{\mathrm{Q}} \sum\nolimits_{q_3=0}^{\mathrm{Q}} \mathbf{D}(w_{q_2})\, \mathbf{D}(w_{q_3})\, \mathbf{U}(n),$$

$$\mathbf{h}_{srd}(n) = \mathbf{H}_{rd,q_3}^{(0)}(n)\, \mathbf{h}_{sr,q_2}(n)$$

and

$$\mathbf{n}_{srd}(n) = \left(\frac{\sqrt{G_{rd}E_s}\mathbf{\Phi}(n)\, \mathbf{n}_{sr}(n)}{\mathbb{E}_{\mathbf{n}_{sr},\mathbf{\Phi}}\left[|\mathbf{y}_{sr}(n)|^2\right]} + \mathbf{n}_{rd}(n) \right) \Big/ \mathbf{\Omega}(n)$$

with $\mathbf{\Omega}(n) = 0.5\sqrt{1 + G_{rd}E_s|\mathbf{\Phi}_{rd}(n)|^2 / \mathbb{E}_{\mathbf{n}_{sr},\mathbf{\Phi}}[|\mathbf{y}_{sr}(n)|^2]}$ and $\mathbf{n}_{rd}(n)$ being the AWGN vector entries of zero mean and $N_0/2$ variance. Arranging (5) and (6) in a matrix form

$$\mathbf{Y}(n) = \mathbf{S}(n)\, \mathbf{h}(n) + \mathbf{n}(n) \tag{7}$$

where $\mathbf{Y}(n) = \left[\ \mathbf{y}_{sd}(n)\quad \mathbf{y}_{rd}(n)\ \right]^{\mathrm{T}}$, $\mathbf{S}(n) = \sqrt{E_s}\mathrm{diag}\left(\mathbf{\Phi}(n), K(n)\mathbf{\Phi}_{srd}(n)\right)$, $\mathbf{h}(n) = \left[\ \mathbf{h}_{sd}(n)\quad \mathbf{h}_{srd}(n)\ \right]^{\mathrm{T}}$ and $\mathbf{n}(n) = \left[\ \mathbf{n}_{sd}(n)\quad \mathbf{n}_{srd}(n)\ \right]^{\mathrm{T}}$. The received signals are then fed to an ML detector.

For the multiple antenna deployment and using the coding scheme presented in Table-1, during the first transmission phase (broadcasting-1), the source vehicle broadcasts two precoded blocks, $\mathbf{u}(n-1) = \mathbf{\Theta}\mathbf{s}(n-1)$ and $\mathbf{u}(n) = \mathbf{\Theta}\mathbf{s}(n)$, from the first and second antennas, respectively. During the second transmission phase (broadcasting-2), the source vehicle broadcasts another version of the two precoded blocks, $\mathbf{u}^*(n) = -\mathbf{\Theta}\mathbf{s}^*(n)$ and $\mathbf{u}^*(n-1) = \mathbf{\Theta}\mathbf{s}^*(n-1)$, from the first and second antennas, respectively. In the third and fourth transmission phases (relaying-1/2), the relay first scales the received signal and then forwards the resulting signal to the destination. Where we re-define the entries in (7) as

$$\mathbf{S}(n) = \left[\ \mathbf{S}_1(n)\quad \mathbf{S}_2(n)\ \right], \quad \mathbf{h}(n) = \left[\ \mathbf{h}_1(n)\quad \mathbf{h}_2(n)\ \right]^{\mathrm{T}}$$

and the rest of the entries is shown in the next page.

$$\mathbf{Y}(n) = \left[\begin{array}{cccccccc} \mathbf{y}_{sd,1}(n-1) & \mathbf{y}_{sd,2}(n-1) & \mathbf{y}_{sd,1}(n) & \mathbf{y}_{sd,2}(n) & \mathbf{y}_{rd,1}(n-1) & \mathbf{y}_{rd,2}(n-1) & \mathbf{y}_{rd,1}(n) & \mathbf{y}_{rd,2}(n) \end{array} \right]^{\mathrm{T}},$$

$$\mathbf{n}(n) = \left[\begin{array}{cccccccc} \mathbf{n}_{sd}^{(1)}(n-1) & \mathbf{n}_{sd}^{(2)}(n-1) & \mathbf{n}_{sd}^{(1)}(n) & \mathbf{n}_{sd}^{(2)}(n) & \tilde{\mathbf{n}}_{rd}^{(1)}(n-1) & \tilde{\mathbf{n}}_{rd}^{(2)}(n-1) & \tilde{\mathbf{n}}_{rd}^{(1)}(n) & \tilde{\mathbf{n}}_{rd}^{(2)}(n) \end{array} \right]^{\mathrm{T}}$$

The related variables are further defined as follows

$$\mathbf{h}_a(n) = \left[\begin{array}{cccc} \mathbf{h}_{sd}^{(a,1)}(n-1) & \mathbf{h}_{sd}^{(a,2)}(n-1) & \left(\mathbf{h}_{sd}^{(a,1)}(n)\right)^* & \left(\mathbf{h}_{sd}^{(a,2)}(n)\right)^* \\ \mathbf{H}_{rd}^{(1,1)}(n-1)\mathbf{h}_{sr}^{(a,1)}(n-1) & \mathbf{H}_{rd}^{(1,2)}(n-1)\mathbf{h}_{sr}^{(a,1)}(n-1) & \mathbf{H}_{rd}^{(1,1)}(n)\left(\mathbf{h}_{sr}^{(a,1)}(n)\right)^* & \mathbf{H}_{rd}^{(1,2)}(n)\left(\mathbf{h}_{sr}^{(a,1)}(n)\right)^* \end{array} \right]^{\mathrm{T}},$$

$$\begin{aligned} \mathbf{S}_1(n) = \mathrm{diag}\Big(& \sqrt{G_{sd}/2}\mathbf{\Phi}_{sd}^{(1,1)}(n-1), \sqrt{G_{sd}/2}\mathbf{\Phi}_{sd}^{(1,2)}(n-1), -\sqrt{G_{sd}/2}\mathbf{\Phi}_{sd}^{(1,1)}(n), -\sqrt{G_{sd}/2}\mathbf{\Phi}_{sd}^{(1,2)}(n), \\ & K_1(n-1)\mathbf{\Phi}_{srd}^{(1,1)}(n-1), K_2(n-1)\mathbf{\Phi}_{srd}^{(1,2)}(n-1), -K_1(n)\mathbf{\Phi}_{srd}^{(1,1)}(n), -K_2(n)\mathbf{\Phi}_{srd}^{(1,2)}(n)\Big), \\ \mathbf{S}_2(n) = \mathrm{diag}\Big(& \sqrt{G_{sd}/2}\mathbf{\Phi}_{sd}^{(2,1)}(n), \sqrt{G_{sd}/2}\mathbf{\Phi}_{sd}^{(2,2)}(n), \sqrt{G_{sd}/2}\mathbf{\Phi}_{sd}^{(2,1)}(n-1), \sqrt{G_{sd}/2}\mathbf{\Phi}_{sd}^{(2,2)}(n-1), \\ & K_1(n-1)\mathbf{\Phi}_{srd}^{(2,1)}(n), K_2(n-1)\mathbf{\Phi}_{srd}^{(2,2)}(n), K_1(n)\mathbf{\Phi}_{srd}^{(2,1)}(n), K_2(n)\mathbf{\Phi}_{srd}^{(2,2)}(n)\Big), \end{aligned}$$

where

$$\begin{aligned} \mathbf{\Phi}_{sr}^{(a,b)}(.) &= \left[\begin{array}{cccc} \mathbf{D}(w_0)\mathbf{\Upsilon}_a\mathbf{U}_{sr}^{(a,b)}(.), & \ldots & , \mathbf{D}(w_{\mathrm{Q}})\mathbf{\Upsilon}_a\mathbf{U}_{sr}^{(a,b)}(.) \end{array} \right], \\ \mathbf{\Phi}_{srd}^{(a,b)}(.) &= \sum_{q_2=0}^{\mathrm{Q}}\sum_{q_3=0}^{\mathrm{Q}}\mathbf{D}(w_{q_2})\mathbf{D}(w_{q_3})\mathbf{\Upsilon}_a\mathbf{U}_{sr}^{(a,b)}(.), \end{aligned}$$

$$K_b(.) = \sqrt{\frac{G_{sr}G_{rd}}{2\mathbb{E}_{\mathbf{n}_{sr},\mathbf{\Phi}}\left[|\mathbf{y}_{sr,b}(.)|^2\right]}\left(\frac{G_{rd}\mathbb{E}\left|\sum_{q=0}^{\mathrm{Q}}\mathbf{D}(w_q)\mathbf{\Upsilon}_1\mathbf{H}_{rd,q}^{(1,b)}(.)\right|^2}{G_{rd}\sqrt{\frac{E_s}{2}}\mathbb{E}\left|\sum_{q=0}^{\mathrm{Q}}\mathbf{D}(w_q)\mathbf{\Upsilon}_1\mathbf{H}_{rd,q}^{(1,b)}(.)\right|^2 + 2\mathbb{E}_{\mathbf{n}_{rd},\mathbf{\Phi}}\left[|\mathbf{y}_{rd,b}(.)|^2\right]}\right)}$$

$$\tilde{\mathbf{n}}_{rd}^{(b)}(.) = \sqrt{\frac{G_{rd}\sqrt{\frac{E_s}{2}}\mathbb{E}\left|\sum_{q=0}^{\mathrm{Q}}\mathbf{D}(w_q)\mathbf{\Upsilon}_1\mathbf{H}_{rd,q}^{(1,b)}(.)\right|^2}{G_{rd}\sqrt{\frac{E_s}{2}}\mathbb{E}\left|\sum_{q=0}^{\mathrm{Q}}\mathbf{D}(w_q)\mathbf{\Upsilon}_1\mathbf{H}_{rd,q}^{(1,b)}(.)\right|^2 + 2\mathbb{E}_{\mathbf{n}_{rd},\mathbf{\Phi}}\left[|\mathbf{y}_{rd}(.)|^2\right]}}\left(\frac{\sqrt{G_{rd}}\mathbb{E}\left|\sum_{q=0}^{\mathrm{Q}}\mathbf{D}(w_q)\mathbf{\Upsilon}_1\mathbf{H}_{rd,q}^{(1,b)}(.)\right|^2}{\sqrt{\mathbb{E}_{\mathbf{n}_{sr},\mathbf{\Phi}}\left[|\mathbf{y}_{sr}(.)|^2\right]}}\mathbf{n}_{sr}(.) + \mathbf{n}_{rd}^{b}(.)\right)$$

with $a, b \in \{1, 2\}$

III. PEP Derivation and Diversity Gain Analysis

In this section, we investigate the achievable diversity gain for our two phases dual-hop cooperative MIMO deployment through the derivation of the PEP. We assume perfect CSI at the relay and receiver sides. Let $\hat{\mathbf{S}}$ represent the erroneously decoded data matrix instead of the originally transmitted $\mathbf{S}$. After dropping the block index n in for convenience of the presentation, the conditional PEP is given by [15]

$$P(\mathbf{S} \to \hat{\mathbf{S}} \Big| \mathbf{h}) = Q\left(\sqrt{\frac{1}{2N_0}d^2\left(\mathbf{S}, \hat{\mathbf{S}}\Big|\mathbf{h}\right)}\right) \qquad (8)$$

Using the lower bounds recently proposed in [16], (8) can be tightly lower bounded by

$$P\left(\mathbf{S} \to \hat{\mathbf{S}}\Big|\mathbf{h}\right) \approx \sum_{m=1}^{3}\varepsilon_m \exp\left(-\frac{\rho_m}{4N_0}d^2\left(\mathbf{S}, \hat{\mathbf{S}}\Big|\mathbf{h}\right)\right) \qquad (9)$$

where $\varepsilon_1 = \varepsilon_2 = 2\varepsilon_3 = 1/12$, $\rho_1 = 12\left(\sqrt{3}-1\right)/\pi$, $\rho_2 = 4\left(3-\sqrt{3}\right)/\pi$ and $\rho_3 = 2\sqrt{3}/\pi$. In the above, the Euclidean distance conditioned on the fading channel coefficients is $d^2\left(\mathbf{S} \to \hat{\mathbf{S}}\Big|\mathbf{h}\right) = \mathbf{h}^{\mathrm{H}}\mathbf{\Delta}\mathbf{h}$ with $\mathbf{\Delta} = \left(\mathbf{S}-\hat{\mathbf{S}}\right)^{\mathrm{H}}\left(\mathbf{S}-\hat{\mathbf{S}}\right)$. Define $\gamma = E_s/N_0$ as the signal-to-noise ratio (SNR). After dropping the block indices $n-1$ and n in for convenience of the presentation, the exact PEP is given by (8) and the $\mathbf{S}$ matrix that holds the transmitted data information is now

represented in terms of $\mathbf{S}_1$ and $\mathbf{S}_2$ earlier defined. The Euclidean distance conditioned on the fading channel coefficients is $d^2\left(\mathbf{S}\to\hat{\mathbf{S}}\middle|\,\mathbf{h}\right) = \mathbf{h}_1^{\mathrm{H}}\boldsymbol{\Delta}_1\mathbf{h}_1 + \mathbf{h}_2^{\mathrm{H}}\boldsymbol{\Delta}_2\mathbf{h}_2 + \mathbf{h}_1^{\mathrm{H}}\boldsymbol{\Delta}_3\mathbf{h}_2 + \mathbf{h}_2^{\mathrm{H}}\boldsymbol{\Delta}_4\mathbf{h}_1$ where $\boldsymbol{\Delta}_1 = \left(\mathbf{S}_1-\hat{\mathbf{S}}_1\right)^{\mathrm{H}}\left(\mathbf{S}_1-\hat{\mathbf{S}}_1\right)$, $\boldsymbol{\Delta}_2 = \left(\mathbf{S}_2-\hat{\mathbf{S}}_2\right)^{\mathrm{H}}\left(\mathbf{S}_2-\hat{\mathbf{S}}_2\right)$, $\boldsymbol{\Delta}_3 = \left(\mathbf{S}_1-\hat{\mathbf{S}}_1\right)^{\mathrm{H}}\left(\mathbf{S}_2-\hat{\mathbf{S}}_2\right)$ and $\boldsymbol{\Delta}_4 = \left(\mathbf{S}_2-\hat{\mathbf{S}}_2\right)^{\mathrm{H}}\left(\mathbf{S}_1-\hat{\mathbf{S}}_1\right)$. Defining $\boldsymbol{\chi}_{a,b}(\mathcal{J}) = ([\hat{\mathbf{S}}_a^{\mathrm{H}}]_{\mathcal{J},\mathcal{J}}-[\hat{\mathbf{S}}_b^{\mathrm{H}}]_{\mathcal{J},\mathcal{J}})([\hat{\mathbf{S}}_a]_{\mathcal{J},\mathcal{J}}-[\hat{\mathbf{S}}_b]_{\mathcal{J},\mathcal{J}})$, where $\mathcal{J}\in\{1,2,\dots N_t\}$ and $a,b\in\{1,2\}$, we can rewrite (9) as

$$P\left(\mathbf{S}\to\hat{\mathbf{S}}\middle|\,\mathbf{h}_1,\mathbf{h}_2\right)\approx \sum_{m=1}^{3}\varepsilon_m\exp\left(-\gamma\tfrac{\rho_m}{4}\left(\sum_{a=1}^{2}\sum_{b=1}^{2}\mathbf{h}_a^{\mathrm{H}}\boldsymbol{\chi}_{a,b}\mathbf{h}_b\right)\right) \tag{10}$$

we need to average (10) over $\mathbf{h}_1$ and $\mathbf{h}_2$. Using the eigenvectors decomposition for the channel vectors $\mathbf{h}_{sd}^{(a,b)}(n-1)$ and $\mathbf{h}_{sd}^{(a,b)}(n)$, we have

$$\begin{aligned}P&\left(\mathbf{S}\to\hat{\mathbf{S}}\middle|\,[\mathbf{h}_1]_{c,1},[\mathbf{h}_2]_{c,1}\atop c\in\{5,6,7,8\}\right)\\ &\approx\sum_{m=1}^{3}\varepsilon_m\exp\left(-\gamma\tfrac{\rho_m}{4}\left(\sum_{a=1}^{2}\sum_{b=1}^{2}\mathbf{h}_a^{\mathrm{H}}\boldsymbol{\chi}_{a,b}\mathbf{h}_b\right)\right)\\ &\times\left(\sum_{l=1}^{2}\prod_{e(l)=1}^{4}\prod_{p_{e(l)}=0}^{r_{e(l)}-1}\left(\frac{4}{4+\rho_m\sqrt{G_{sd}/2}\lambda_{p_{e(l)}}\gamma}\right)\right)\end{aligned} \tag{11}$$

where the indices $e(l)\in\{1,2,3,4\}$ are associated sequentially for autocorrelation matrices $\mathbf{C}_{h,sd}^{(a,b)} := \mathbb{E}[(\mathbf{h}_{sd}^{(a,b)})^{\mathrm{H}}\mathbf{h}_{sd}^{(a,b)}]$ with ranks $r_{e(l)}$. The eigenvector entries for the associated links are given by $\lambda_{p_{e(l)}}$. We now need to average (11) over $\mathbf{H}_{rd}^{(1,b)}(n-1)\,\mathbf{h}_{sr}^{(a,1)}(n-1)$ and $\mathbf{H}_{rd}^{(1,b)}(n)\,(\mathbf{h}_{sr}^{(a,1)}(n))^*$. Following similar steps as in [17], we obtain the unconditional PEP as shown in (12), with the rank of the associated channels autocorrelation matrices as $r_{\mathfrak{g}(k)}$. We have $\delta_{j_{\mathfrak{g}(k)}} = \exp\left(-4\kappa_{j_{\mathfrak{g}(k)}}/\left(K_k^2\rho_m\gamma\right)\right)\Big/\prod_{k\neq j,k=0}^{r_{\mathfrak{g}(k)}-1-p_3}(\kappa_k-\kappa_j)$ and $\Gamma(0,x)$ is the incomplete gamma function.

The eigenvector entries for the associated links given by $\kappa_{i_{\mathfrak{g}(k)}}$. From (12), we observe an asymptotical diversity gain

$$\min_{l\in\{1,2\}}\left(r_{e(l)}\right)+\min_{k\in\{1,2\}}\left(r_{\mathfrak{g}(k)}\right) = \sum_{a=1}^{2}\sum_{b=1}^{2}\left(\left(L_{sd}^{a,b}+1\right)\left(Q_{sd}^{a,b}+1\right)\right)+4 \tag{13}$$

From (13), we observe a maximum asymptotical diversity gain is bounded by the rank of the auto-correlation matrix associated with the direct link (S→D) and the minimum of the cooperative relaying links (S→R and R→D), taking into consideration the number of transmit and receive antennas involved in the transmission. If the relative traveling velocity of relaying vehicle with respect to the designated vehicle is not equal to zero, extra diversity gains can be extracted from the S→R→D link.

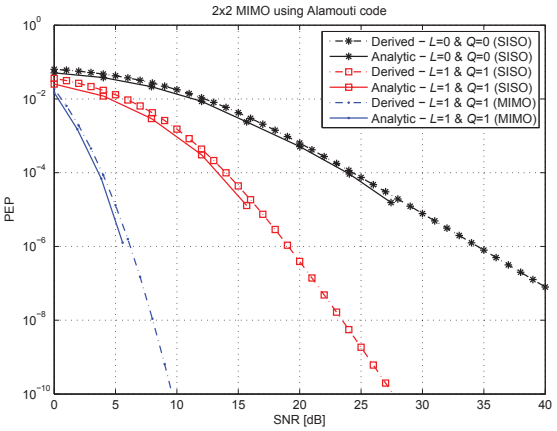

Fig. 2: Comparison of derived (13) and analytical PEPs (8).

IV. Numerical Results and Discussion

In this section, we demonstrate the performance gains of the proposed scheme. As defined in the standard, LTE-A targets peak data rates up to 1 Gb/s with up to 100 MHz supported spectrum bandwidth and QPSK modulation is used. Unless otherwise stated, we consider $f_c = 2.5$ GHz, $\mathrm{T_s} = 500\ \mu s$, $v_r = v_d = 120$km/h, $\alpha = 3.67$, $\theta = \pi$, $G_{sr}/G_{rd} = -30$ dB and $\tau_d = 1.328\ \mu$s [18]. We assume perfect channel state information is available at the receiving terminals. We use the precoder $\boldsymbol{\Theta}$ with parameters $P = 2$ and $Z = 2$. This results in $[L_{sd}, Q_{sd}] = [1,1]$ for S → D link. Due to the zero relative velocity for the R → D link, a frequency-time flat channel is used, hence $[L_{coop}, Q_{coop}] = [0,0]$.

In Fig-2 we verify our closed-form expression derivation by comparing the derived PEP expressions for (12) with the exact (analytical) PEP expressions. Analytical PEP can be found by taking the expectation numerically for (8), through random generation of all the underlying $\mathbf{h}_{sd}$, $\mathbf{h}_{sr}$ and $\mathbf{h}_{rd}$ links, and using proper statistics via numerical techniques. We observe that as (L) and/or (Q) increase, significant improvements are observed through precoding that takes advantages of diversity gains. For example at a target pair wise error rate of 10^{-4}, the precoded system over a channel with $L = 1$ and $Q = 1$ (with a single antenna deployment 'SISO') is 10 dB superior to the benchmark curve of $L = 0$ and $Q = 0$. The bench mark curve indicates the un-precoded flat channels, with a single antenna deployment. Performance improvement climbs up to 20 dB for $L = 1$ and $Q = 1$ with our proposed transmission scheme (2X2 MIMO with Alamouti STBC).

In Fig-3 we plot the slope of our proposed scheme to precisely observe the attained gain. The achieved diversity orders is consistent with (13) and equal to $D_{gain,R} = 20$, compared to $D_{gain,R} = 2$ for traditional unprecoded cooperative relaying transmission and $D_{gain,R} = 5$ for the precoded cooperative relaying transmission with single antenna deployment.

Finally, we remark that there are mainly two approaches to extract multipath-Doppler diversity on doubly-selective fading channels. The first approach involves adaptive transmission

$$P_m\left(\mathbf{S}\to\hat{\mathbf{S}}\right)\approx\sum_{m=1}^{3}\varepsilon_m\left(\sum_{l=1}^{2}\prod_{e(l)=1}^{4}\prod_{p_{e(l)}=0}^{r_{e(l)}-1}\left(\frac{4}{4+\rho_m\sqrt{G_{sd}/2}\lambda_{p_{e(l)}}\gamma}\right)\right)$$
$$\times\left(\sum_{k=1}^{2}\prod_{\mathfrak{g}(k)=5}^{8}\left(\prod_{p_2=0}^{r_{\mathfrak{g}(k)}-1}\frac{4}{\rho_m K_k^2\gamma}\left(\prod_{p_3=0}^{r_{\mathfrak{g}(k)}-1}\left(\prod_{i_{\mathfrak{g}(k)}=0}^{r_{\mathfrak{g}(k)}-1-p_3}\kappa_{i_{\mathfrak{g}(k)}}\sum_{j_{\mathfrak{g}(k)}=0}^{r_{\mathfrak{g}(k)}-1-p_3}\left(\delta_{j_{\mathfrak{g}(k)}}\Gamma\left(0,\frac{4\kappa_{j_{\mathfrak{g}(k)}}}{K_k^2\rho_m\gamma}\right)\right)\right)\right)\right)\right)\right) \tag{12}$$

where $\mathbf{R}_{h,srd}^{(a,b)}(n-1):=\mathbb{E}[(\mathbf{H}_{rd}^{(1,b)}(n-1)\mathbf{h}_{sr}^{(a,1)}(n-1))^{\mathrm{H}}(\mathbf{H}_{rd}^{(1,b)}(n-1)\mathbf{h}_{sr}^{(a,1)}(n-1))]$

and $\mathbf{R}_{h,srd}^{(a,b)}(n):=\mathbb{E}[(\mathbf{H}_{rd}^{(1,b)}(n)(\mathbf{h}_{sr}^{(a,1)}(n))^*)^{\mathrm{H}}(\mathbf{H}_{rd}^{(1,b)}(n)(\mathbf{h}_{sr}^{(a,1)}(n))^*)]$

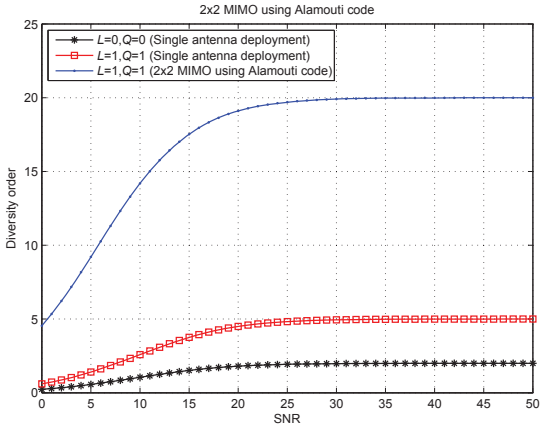

Fig. 3: Diversity order for the MIMO cooperative relaying.

techniques in which one or more transmission parameters (coding, modulation, power etc) are varied according to the channel conditions. This builds on a closed-loop implementation in which a feedback from the receiver to the transmitter is required. The second approach is the use of either outer coding or precoding techniques. These are open-loop implementations and do not require feedback. Such techniques are particularly useful over time-varying channels where reliable feedback is difficult to obtain.

V. Conclusion

We have investigated the performance of vehicular relaying for an LTE-A downlink with a STBC-MIMO deployment session communicating with a designated traveling vehicle. To extract the underlying rich multipath-Doppler-spatial diversity over the doubly-selective relaying channel, we take advantage of a precoded cooperative transmission with a multiple antenna deployment at the BS side and at the designated vehicle. Our findings demonstrate an improvement to the error rate performance and that a full diversity gains is achievable through proper precoding. We have presented numerical and simulation results for error rate performance to confirm the analytical derivations if properly exploited, the performance can be improved for channels with higher time-spectral variations.

Acknowledgement

This work was made possible by a *National Priorities Research Program* (NPRP) grant from the Qatar National Research Fund (Member of Qatar Foundation).

References

[1] S. Zeadally, R. Hunt, Y. Chen, A. Irwin and A. Hassan, "Vehicular ad hoc networks (VANETS): status, results, and challenges," J. Telecommun. Syst., Vol. 50, no. 4, pp. 217-241, Aug 2012.

[2] P. L. M. Pan, "Cooperative Communication Aware Link Scheduling for Cognitive Vehicular Networks," *IEEE J. Sel. Areas Comm.*, vol. 30, no.4, pp. 760-768, 2012.

[3] M. Nazirah, A. Izzati, N. Fisal, S. K. S. Yusof, S. H. S. Ariffin and M. Abbas, "Cross-layer routing approach in high speed mobile wireless networks," in *Proc. 9th Int. Conf. Syst. Sci. and Simu. Eng.*, WSEAS'2010, pp. 238-243.

[4] T. P. Ren, Y. L. Guan, C. Yuen and R. J. Shen, "Delay-tolerant cooperative diversity routing MANET," in *IEEE 72nd Veh. Technol. Conf.*, VTC, 2010, pp. 1-5.

[5] S. C. H. Jang, "Cooperative transmission aid in intermittent broken connection on VANET," in *10th Int. Symp. Pervasive Syst. Algorithms and Networks*, ISPAN, 2009, pp. 620-624.

[6] H. Ilhan, M. Uysal and . Altunbas, "Cooperative Diversity for Intervehicular Communication: Performance Analysis and Optimization," *IEEE Trans. Veh. Technol.*, vol. 58, pp. 3301-3310, 2009.

[7] M. F. Feteiha and H. Hassanein, "Cooperative vehicular relaying in LTE-A networks," in *9th Int Wireless Commun. Mobile Comput. Conf.*, IWCMC, Sardinia, Italy, 2013.

[8] M. F. Feteiha, H. Hassanein and Kubbar, "Opportunistic cooperation for infrastructure-to-relaying-vehicles over LTE-A networks," in *Int. Conf. Commun.*, ICC, Budapest, Hungary, 2013.

[9] S. M. Alamouti, "A simple transmit diversity technique for wireless communications," *IEEE J. Select. Areas Commun.*, vol. 16, pp. 1451-1458, 1998.

[10] X. Ma, G. Leus and G. B. Giannakis, "Space-time-Doppler block coding for correlated time-selective fading channels," *IEEE Trans. Signal Process.*, vol. 53, pp. 2167-2181, 2005.

[11] B. Talha and M. Patzold, "Channel models for mobile-to-mobile cooperative communication systems," *IEEE Veh. Technol. Mag.*, vol.6, no. 2, pp. 33-43, June 2011.

[12] J. Laneman, D. Tse and G. Wornell, "Cooperative diversity in wireless networks: Efficient protocols and outage behavior," *IEEE Trans. Inf. Theory*, vol. 50, no. 12, pp. 3062-3080, Jun 2004.

[13] X. Ma and G. Giannakis, "Maximum-diversity transmissions over doubly selective wireless channels," *IEEE Trans. Inf. Theory*, vol. 49, pp. 1832-1840, 2003.

[14] R. U. Nabar, H. Bolcskei and F. W. Kneubuhler, "Fading relay channels: Performance limits and space-time signal design," *IEEE J. Select. Areas Commun.*, vol. 22, pp. 1099-1109, 2004.

[15] V. Tarokh, N. Seshadri and A. Calderbank, "Space-time codes for high data rate wireless communication: Performance criterion and code construction," *IEEE Trans. Inf. Theory*, vol. 44, pp. 744-765, 1998.

[16] M. Wu, X. Lin and P. Y. Kam, "New exponential lower bounds on the gaussian Q-function via jensen's inequality," in *IEEE 73rd Veh. Technol. Conf.*, VTC'11, Budapest, Hungary, pp. 1-5, May 2011.

[17] M. F. Feteiha and M. Uysal ,"Cooperative Transmission for Broadband Vehicular Networks over Doubly-Selective Fading Channels," *J. IET Commun.*, vol. 6, no. 16, pp. 2760-2768, Nov 2012.

[18] C. Zhang, S. Ariyavisitakul and M. Tao, "LTE-advanced and 4G wireless communications [Guest Editorial]," *IEEE Commun. Mag.*, vol. 50, pp. 102-103, 2012.